

Mechano-transduction of DNA hybridization and dopamine oxidation through electrodeposited chitosan network†

Stephan T. Koev,^{ab} Michael A. Powers,^{ab} Hyunmin Yi,^c Li-Qun Wu,^d William E. Bentley,^{def} Gary W. Rubloff,^{bfg} Gregory F. Payne^{df} and Reza Ghodssi^{*abf}

Received 28th June 2006, Accepted 3rd October 2006

First published as an Advance Article on the web 17th October 2006

DOI: 10.1039/b609149k

While microcantilevers offer exciting opportunities for mechano-detection, they often suffer from limitations in either sensitivity or selectivity. To address these limitations, we electrodeposited a chitosan film onto a cantilever surface and mechano-transduced detection events through the chitosan network. Our first demonstration was the detection of nucleic acid hybridization. In this instance, we electrodeposited the chitosan film onto the cantilever, biofunctionalized the film with oligonucleotide probe, and detected target DNA hybridization by cantilever bending in solution (static mode) or resonant frequency shifts in air (dynamic mode). In both detection modes, we observed a two-order of magnitude increase in sensitivity compared to values reported in literature for DNA immobilized on self-assembled monolayers. In our second demonstration, we coupled electrochemical and mechanical modes to selectively detect the neurotransmitter dopamine. A chitosan-coated cantilever was biased to electrochemically oxidize dopamine solution. Dopamine's oxidation products react with the chitosan film and create a tensile stress of approximately 1.7 MPa, causing substantial cantilever bending. A control experiment was performed with ascorbic acid solution. It was shown that the electrochemical oxidation of ascorbic acid does not lead to reactions with chitosan and does not change cantilever bending. These results suggest that chitosan can confer increased sensitivity and selectivity to microcantilever sensors.

1. Introduction

Microfabricated cantilevers are emerging as important analytical tools for chemical and biological detection.^{1–15} Two approaches are commonly used to functionalize the cantilever surface to allow chemical or biological information to be “recognized” and mechano-transduced. One functionalization approach employs self-assembled monolayers (SAMs) to attach ligands to one of the cantilever's surfaces.^{3,5,12,14} Binding of target molecules to this cantilever-bound ligand generates surface stresses that are transmitted to the cantilever. SAM-functionalized cantilevers are commonly considered for detecting biomolecular recognition events (e.g., antigen–antibody binding or nucleic acid hybridization). While these

biological ligands confer high selectivity, mechano-transduction of the recognition event is often limited. A second functionalization approach is to couple responsive polymeric networks to cantilevers. These networks swell or collapse in response to chemical stimuli, and these responses are transmitted to the cantilever.^{7–10,16} Typically, polymer-based cantilevers (or cantilever arrays) are considered for detecting differences in salt, humidity and vapor composition. While these polymeric networks can generate considerable surface stresses for mechano-transduction, they typically offer limited selectivity. Here, we report a hybrid approach based on the amino-polysaccharide chitosan.

Chitosan has three important properties that make it uniquely suited as a bio-device interface material.^{17,18} Chitosan is stimuli-responsive and undergoes a soluble-to-insoluble transition in response to a pH switch from 6 to 6.5. Chitosan is also film-forming such that this pH switch can generate a stable hydrogel network. These two properties—pH-responsive and film-forming—allow stable chitosan films to be electrodeposited at cathode surfaces.^{19,20} The pH-switching at the cathode surface is easily controlled, and chitosan can be electrodeposited with high spatial²¹ and temporal²² control. Interestingly, due to the stability of the chitosan film, various components can be co-deposited with chitosan and entrapped within its hydrogel network.^{23–25} Chitosan's third unique property is that it is nucleophilic. Chemically, chitosan has primary amines at nearly every repeating unit of its polymeric structure. These amines are

^aDepartment of Electrical and Computer Engineering, University of Maryland, College Park, MD, 20742, USA.
E-mail: ghodssi@eng.umd.edu; Fax: 1-301-314-9218;
Tel: 1-301-405-8158

^bInstitute for Systems Research, College Park, MD, 20742, USA

^cDepartment of Chemical and Biological Engineering, Tufts University, Medford, MA 02155, USA

^dUniversity of Maryland Biotechnology Institute, College Park, MD, 20742, USA

^eDepartment of Chemical Engineering, College Park, MD, 20742, USA

^fBioengineering Graduate Program, University of Maryland, College Park, MD, 20742, USA

^gDepartment of Materials Science and Engineering, College Park, MD, 20742, USA

† Electronic supplementary information (ESI) available: Additional chemical evidence, UV/vis spectra and a table of properties. See DOI: 10.1039/b609149k

nucleophilic and readily react with electrophiles. For instance, we have used standard glutaraldehyde-based coupling chemistries to bio-functionalize electrodeposited films with biological components (*e.g.*, proteins,²⁶ nucleic acids,²⁷ and virus particles²⁸). In sum, previous results have shown that chitosan can perform two functions at the interface—it can be directed to assemble (*i.e.*, electrodeposit) in response to localized signals, and it can be functionalized through standard chemistries. Here, we report a third function: chitosan networks can transmit mechanical information of chemical and biological events to the cantilever surface.

We examined two model experimental systems to demonstrate chitosan's mechano-transduction function. Our first demonstration is the detection of DNA hybridization, which is a “conventional” application for microcantilever mechanosensors.^{5,12,14,15,29,30} For this demonstration, we employ chitosan's stimuli-responsive and film-forming properties for electrodeposition on the cantilever, after which we employ chitosan's nucleophilic properties to functionalize the film with an oligonucleotide-probe. Hybridization of this probe with a complementary target DNA is detected as a differential deflection when measured in solution (static mode), or a resonant frequency shift when measured in air (dynamic mode).

Our second demonstration of chitosan's mechano-transduction function is a novel one, and it couples electrochemical and mechanical modes to selectively detect the neurotransmitter dopamine. Dopamine and related catechols are readily oxidized; interestingly, oxidized catechols are electrophilic and react with chitosan.³¹ In some cases, oxidized catechols can covalently crosslink chitosan and substantially alter its mechanical properties.³² For our second demonstration, this change in mechanical properties of chitosan films due to dopamine oxidation is detected by the differential deflection of microcantilevers (static mode). Biological samples often contain components such as ascorbic acid that are also easily oxidized and interfere with the dopamine detection.^{33,34} We show that the mechano-detection method can successfully discriminate between dopamine and ascorbic acid solutions.

2. Materials and methods

2.1. Cantilever design

For the static mode of operation, chitosan must be electrodeposited on only one side of the cantilever in order to create a differential surface stress and bending. This requirement dictates that only one surface of the cantilever is conductive, and the cantilever material is insulating. For the dynamic (resonant) mode of operation in this work, the cantilever must be insulated from the substrate to enable electrostatic actuation. The selected materials and fabrication process meet both of these requirements, enabling the same device to be used in both static and dynamic testing.

The microcantilever sensor consists of layers of chitosan (varying thickness), Au (80 nm), Cr (20 nm), and Si₃N₄ (500 nm), on a Si substrate with a SiO₂ layer (500 nm). The length of the released beam is 100 μm, and the width is 40 μm. The air gap (distance between cantilever bottom and substrate)

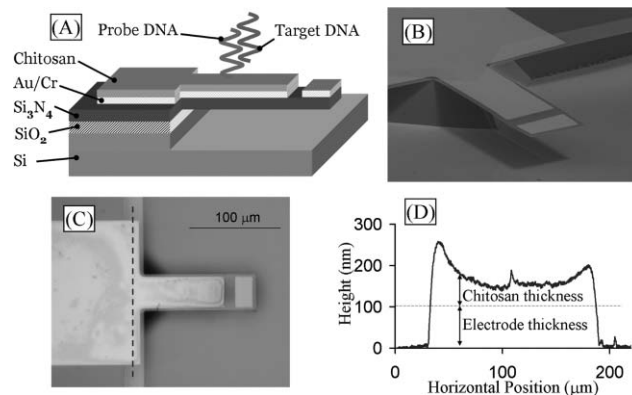


Fig. 1 (A) Cross sectional schematic of microcantilever with chitosan used for detection of DNA hybridization and for detection of dopamine electrochemical oxidation. (B) SEM of fabricated cantilever. The (111) silicon crystallographic planes are sloped and visible near the cantilever base. (C) Optical micrograph of cantilever after chitosan electrodeposition. The chitosan is deposited everywhere except at the electrically isolated tip. (D) Contact profiler scan of chitosan film along dashed line in C. Higher electric field near the edges increases the deposition rate and the resulting chitosan thickness there.

is 20 μm. A cross sectional schematic of the device is shown in Fig. 1A. In both static and dynamic modes, the cantilever displacement is measured using a Veeco NT1100 optical interferometer. In the dynamic mode, the resonant frequency of the cantilever is measured before and after the biomolecular detection event, and the presence of the analyte is inferred from the resonant frequency shift. In this mode, measurements are performed in air after drying the cantilever chip to maximize the resonance quality factor. In the static mode, the bending of the cantilever is measured before and after the detection event, and the presence of the analyte is inferred from the change in bending. In this mode, measurements are taken with the chip immersed in solution.

2.1.1. Dynamic mode analysis. In the dynamic mode of operation, the resonant frequency of the cantilever is measured before and after DNA hybridization to detect the mass change. The fundamental undamped resonant frequency f_{res} of a uniformly loaded cantilever using the standard assumptions of beam theory³⁵ is given by eqn (1). Here, E is Young's modulus; ρ is density; H , L and W are thickness, length and width of the beam respectively; I is the moment of inertia about the cantilever's neutral axis. An effective Young's modulus and effective density are needed in eqn (1) to account for the multiple layers of the cantilever. These quantities can be found from the properties and geometries of each layer as shown by eqn (2) and (3) for N layers.³⁶

$$f_{\text{res}} = 0.56 \sqrt{\frac{EI}{\rho H W L^4}} \quad (1)$$

$$E = \frac{\sum_{i=1}^N E_i I_i}{I} \quad (2)$$

$$\rho = \frac{\sum_{i=1}^N \rho_i H_i}{H} \quad (3)$$

Assuming a small resonant frequency shift Δf_{res} , the sensitivity of the cantilevers to uniformly distributed target loading with surface density σ_t can be shown to be:

$$\frac{\Delta f_{\text{res}}}{\sigma_t} = -\frac{f_{\text{res}}}{2\rho H} C \quad (4)$$

Here, the factor C accounts for incomplete coverage of the cantilever with chitosan and target biomolecules, and it becomes 1 if the whole cantilever is covered. Note from Fig. 1A that the tip of the cantilever has an electrically isolated metal rectangle with an area approximately 20% of the cantilever surface. This rectangle does not experience chitosan deposition and is used for displacement measurements in dynamic mode. Chitosan has a rough surface and typically increases optical measurement error. The factor C in eqn (4) due to the chitosan-free rectangle in this design is 0.31. To maximize sensitivity, the rectangle can be reduced in size or moved to a different location on the cantilever.

Note from eqn (4) that the sensitivity increases with increasing resonant frequency and with decreasing cantilever thickness. However, decreasing the thickness generally leads to a reduction of the quality factor because the ratio of elastic and inertial forces to air damping forces is reduced. This in turn hurts the accuracy of resonant frequency measurements. An optimal design for a cantilever would require empirical knowledge of the Q factor as a function of resonant frequency and thickness. The present design is not optimized for sensitivity but rather for ease of measurement and experimentation. Based on the material properties commonly reported in literature and tabulated in the electronic supplementary information (ESI)† entry for this paper, the calculated resonant frequency is 60 kHz and the sensitivity is 63 Hz cm² μg⁻¹. The contribution of chitosan is ignored in this first-order analysis since the mechanical properties of chitosan and its surface topography vary considerably with deposition conditions.

2.1.2. Static mode analysis. In the static mode of operation, cantilever bending is measured before and after DNA hybridization or dopamine oxidation. The displacement of the tip by surface stress is given by the Stoney equation:³⁷

$$\Delta z = 3\sigma_s \frac{(1-\nu)L^2}{EH^2} \quad (5)$$

Here, σ_s is the surface stress, ν is the Poisson ratio, L is the beam length, and H is the thickness, and E is the effective Young's modulus as defined previously. The Stoney equation is inaccurate for short cantilevers, and several modified equations have been derived.^{37,38} Sader³⁸ showed that the error in cantilever tip displacement given by the Stoney equation is approximately 10% for cantilevers with a length to width ratio of 2.5 (the cantilevers in our work are 100 μm long and 40 μm wide). This error is considered acceptable here and the original Stoney equation is therefore used.

The amount of bending for a given stress increases with length of the cantilever and with reducing thickness. However, as in the case of the dynamic mode operation, other factors such as stiction, cantilever fragility, and ease of measurement were taken into consideration when determining device

dimensions. As a result, the cantilevers used for static operation were designed with the same dimensions as those for dynamic operation. They do not, however, have the isolated metal rectangle at the tip and are entirely covered by chitosan. In static mode, a narrowband illumination source is used for the interferometer, enabling accurate measurements to be taken even with chitosan on the surface.

2.2. Cantilever fabrication

The cantilevers were fabricated by conventional MEMS lithographic and etching techniques. The process begins with an n-type Si wafer (100 orientation, resistivity 0.01 Ω cm) with LPCVD films of SiO₂ and Si₃N₄ (500 nm thick each) on both sides. Next, 20 nm of Cr and 80 nm of Au films are deposited on the Si₃N₄ surface by sputtering. Photoresist is patterned to define the metal layer. Note that the features on the mask are aligned along the [100] direction of the Si wafer (at a 45° angle from the wafer flat). The exposed metal is removed by wet chemical etching. The remaining photoresist is stripped with acetone and a second lithography step is performed to define an RIE etch mask. The exposed Si₃N₄ and SiO₂ films are etched using a CF₄/O₂ RIE chemistry. The remaining photoresist is stripped with acetone and the wafer is cleaned in a Piranha solution. The exposed Si is then etched in a KOH solution (45% wt, 80 °C) to release the cantilevers. The measured etch rate of the (100) crystallographic planes is 0.7 μm min⁻¹. Typically, KOH masks are aligned along the [110] direction to prevent mask undercutting. Here, mask undercutting is desirable and is maximized by aligning the features along [100]. This speeds up the cantilever release and produces an air gap small enough for electrostatic actuation. The resulting cantilever air gap is roughly equal to half the width of the cantilever because the horizontal and vertical etch rates are the same. The (111) planes have a much slower etch rate than the (100) planes and form slopes near the bottom corners of the trenches. Fig. 1B shows the resulting structure. This process causes the released cantilever effective length to be about 20 μm less than the cantilever length defined on the mask.

After KOH etching, the released cantilevers consist of layers of SiO₂, Si₃N₄, and Cr/Au. The SiO₂ is removed in concentrated HF because its residual stress causes the cantilever to bend out of plane considerably. This bending is undesirable, and it interferes with optical displacement measurements. The residual stress of the metal layer also causes some cantilever bending. However, that results in only 1 μm upward displacement of the tip and does not impact the optical measurements.

Finally, the wafer is diced in 3 mm by 25 mm chips to facilitate handling during the multiple biochemical reaction steps. Prior to dicing, the wafer is covered in photoresist (without spinning) to protect the released cantilevers. After dicing, the protective photoresist is removed in acetone, and the majority of cantilevers are observed to be intact.

2.3. Chitosan deposition

The electrodeposition of chitosan on microfabricated electrodes has been presented in detail elsewhere.^{19–21} Briefly,

the deposition is performed by immersing the chip in a chitosan solution and applying a negative potential to the electrodes on the chip relative to a counterelectrode in the solution. A pH gradient is established at the cathode due to net hydrogen ion consumption. Since chitosan is insoluble at pH above 6.5, it solidifies at the cathode surface. The rate of chitosan deposition and the properties of the resulting films depend on the composition of the solution, the voltage applied, and the electrode geometry.

Medium molecular weight chitosan flakes from Sigma Aldrich were used to make an aqueous solution with 0.5% w/v chitosan concentration and pH = 5. The deposition conditions were chosen experimentally to obtain the desired chitosan thickness. In a typical experiment, a voltage of -0.9 V applied for 30 s results in an average film thickness of 100 nm as measured by contact profilometry. The chitosan coverage on the cantilever is not uniform because the electric field and the deposition rate near the electrode edges are higher than in the middle of the electrode. Fig. 1C shows a cantilever after deposition. A representative profile of the chitosan film is given in Fig. 1D. Better uniformity of the film could be obtained by slowing down the deposition but is not necessary for this application. Here, the only role of the chitosan is as an interface for attaching the biomolecules, and its uniformity is not a major concern. The deposited chitosan film has tensile residual stress that causes out-of-plane bending of the cantilever when the sample is dried. In practice, the amount of residual stress depends on the exact deposition conditions and varies between experiments. Based on an average measured displacement of the cantilever tip of 2 μm , the calculated chitosan residual stress is approximately 60 MPa tensile. This out-of-plane bending limits the maximum chitosan thickness that can be deposited on the cantilevers. For bending of more than about 10 μm it becomes impossible to measure the cantilever position with the optical interferometer because of depth-of-focus limitations.

After the deposition, the sample is rinsed and immersed in 1 M NaOH solution for 5 min to neutralize the chitosan film. Finally, the sample is equilibrated in SSC buffer (sodium saline citrate) to bring the pH to 7.1.

2.4. Measurement setup and instrumentation

The measurements of cantilever displacement and resonant frequency are taken with a Veeco NT1100 optical interferometer (Tucson, AZ) with dynamic measurement module. This instrument measures static feature heights by interfering a beam reflected from the sample surface with a beam reflected from a reference mirror, capturing the interferogram by a CCD camera and analyzing it in software. Dynamic measurements can be performed by illuminating a periodically moving structure with a strobe synchronized with the structure's actuation signal. The structure's position at a given voltage, frequency and phase are measured as if the structure were static.

2.4.1. Static mode measurements. As discussed in the introductory section, the cantilever sensor is used both in static and dynamic modes. Measurements are performed in

each case before and after a biological event such as DNA hybridization, denaturation, or dopamine oxidation. In the static mode, the measurement consists of a scan of the sample's topography. The scan shows the height of the cantilever at each point, although knowledge of height of the cantilever tip alone is sufficient for detection. In the static mode, displacement measurements both in air and in solution were taken. Only in-solution measurements are presented here since they allow detection in physiological conditions. Measurements in air showed stronger response but have limited applicability since the device has to be dried. The measurement error was evaluated by taking multiple scans of a single device. The typical standard deviation was approximately 30 nm, caused mainly by perturbations in the liquid medium and misalignment of the sample within the interferometer's field of view.

2.4.2. Dynamic mode measurements. In the dynamic mode, the dried cantilever is electrostatically actuated in air at different frequencies and the tip displacement at each frequency is measured. The driving voltage consists of a 40 V_{pp} sinusoidal signal with a 20 V DC offset, such that the total signal is always positive. The peak-to-peak cantilever displacement at this voltage at resonance is 1 μm , which is comparable to the cantilever thickness and is therefore sufficiently small to ensure that the cantilever behaves as a linear spring. The resulting frequency response is fitted with a Lorentzian function, and the peak parameter from the fit is taken to be the resonant frequency. The large coefficient of determination ($R^2 > 0.999$), suggests that cantilever behaves approximately as a second order linear spring-mass system.

The resonant frequency of bare cantilevers without chitosan was measured to be approximately 58 kHz. The calculated resonant frequency for such cantilevers using eqn (1) is approximately 60 kHz. This close agreement suggests that the material properties, cantilever dimensions and assumptions used in the calculation are approximately valid and allows us to use the sensitivity expression eqn (4). As discussed previously, the mechanical properties of the chitosan film vary considerably with the deposition conditions and a theoretical prediction of the resonant frequency of a cantilever with chitosan was not attempted. However, the measured resonant frequency of the chitosan-coated cantilever in practice is only a few kHz above the resonant frequency of the uncoated cantilever. Therefore, eqn (1) and (4) can be used as approximations for cantilevers with chitosan as well. The quality factor of the cantilever's resonance was measured by dividing the displacement at the resonant frequency by the displacement at DC using the same voltage. The average measured Q factor is 20.

Multiple measurements of a single sample are taken to check for repeatability and determine the error bars on the resonant frequency. In the absence of chitosan, the standard deviation of resonant frequency measurements is 5 Hz. This error is caused mainly by ambient vibrations of the interferometer's stage, which corrupt the frequency response peak. Once chitosan is added to the cantilever, the resonant frequency uncertainty increases considerably because the film absorbs humidity. The standard deviation of resonant frequency measurements taken on 5 different days with chitosan was approximately 100 Hz. Since the shifts due to biological

binding events in our experiments are on the order of kHz, this is an acceptable error. However, to improve the detection limit it would be necessary to reduce the humidity-induced variation of the resonant frequency. For example, a reference cantilever can be used to track the instantaneous humidity, and all resonant frequency measurements can be subtracted from that of the reference cantilever.³⁹ Alternatively, the sensor can be isolated from the environment during measurement to provide more repeatable conditions.

2.5. Conjugation of DNA

2.5.1. Oligonucleotide samples

DNA hybridization on the cantilevers was performed in a sandwich assay format in order to observe the results fluorescently in addition to measuring the cantilever mechanical response. Oligonucleotides with various end modifications were purchased from Gene Probe Technologies (Gaithersburg, MD) and are summarized in Table 1. Two different surface probes are used: one is a sequence from the *dnaK* gene in *E. coli*, and the other encodes a hexahistidine tag common for recombinant proteins. The target DNA has a region complementary to the *dnaK* surface probe and has little homology with the *6xHis* surface probe. The target DNA also has two regions complementary to the sandwich probe sequence, which is fluorescently labeled. Thus, the effective length of the target complex is 110 bases and its effective concentration is 1.5 μM .

2.5.2. Hybridization procedure. The conjugation of probe DNA molecules to chitosan and the subsequent hybridization is described in detail elsewhere.^{22,27} After deposition, the chitosan is reacted with glutaraldehyde solution of concentration 0.05% v/v for 30 min. The glutaraldehyde serves as a coupling agent to conjugate the amine groups of the chitosan to amine groups of the surface probe DNA by forming covalent bonds. Samples are placed in two different probe DNA solutions and allowed to react overnight at 4 °C. After the probe conjugation, the samples are reacted with sodium borohydride (NaBH_4) to convert Schiff bases to more stable secondary amine bonds. The chips are then rinsed and the resonant frequency and bending of the cantilevers are measured in air and in solution respectively. Following this, the samples are placed in a solution containing the target DNA and the sandwich probe and are allowed to hybridize for 30 min at room temperature. The chips are rinsed and cantilever measurements are taken again. The samples are then

subjected to denaturing conditions (4 M urea solution at 80 °C for 30 min) to reverse the hybridization. After denaturation, the chips are rinsed and measured again. The hybridization and denaturation are also confirmed by observing the FITC-labeled sandwich probe by fluorescence microscope.

2.6. Electrochemical oxidation of dopamine

The crosslinking of chitosan by electrochemical oxidation of phenols has been discussed in detail elsewhere.^{31,32} Chitosan is deposited on a cantilever as previously described. The sample is placed in deionized (DI) water and the out-of-plane bending of the cantilever is measured with the optical interferometer. A 0.1 M dopamine solution of pH 7.6 is prepared by dissolving dopamine powder in phosphate buffer. The cantilever with chitosan is placed in the solution and a positive potential of 1 V is applied to it relative to a counterelectrode in the solution for 30 s. After rinsing, the sample is placed in DI water and the bending of the cantilever is measured again. Identical experiments are performed with ascorbic acid solutions instead of dopamine solutions with the same concentration and pH.

3. Results

3.1. Detection of DNA hybridization

3.1.1. Static mode results. Our first demonstration is the mechano-transduction of a bio-molecular recognition event (nucleic acid hybridization). For this, we electrodeposited a thin film of chitosan (200 nm) onto the gold-coated cantilever surface, and then used a standard coupling chemistry to functionalize the film with an oligonucleotide probe for *dnaK* as described in previous sections. The vertical profile in Fig. 2A shows the cantilever undergoes considerable upward bending after functionalization with the probe (note that the bending was measured in solution). This functionalized cantilever was then contacted with the complementary target DNA solution (*dnaK*). After hybridizing for 30 min, the cantilever was rinsed with buffer and the vertical profile measured again. Fig. 2A shows that the hybridization enhances the upward bending of the cantilever with a differential bending (Δz) of ~ 500 nm at the tip. This differential bending can be estimated from eqn (5) to be due to an increased surface stress of 1.2 N m^{-1} . Previous studies have shown that chitosan films functionalized with DNA probes are sufficiently robust that they can be denatured to separate the hybridized duplex and regenerate the chitosan-bound probe.²⁷ Thus, we subjected our cantilever to denaturing conditions (4 M urea at 80 °C for 30 min). After

Table 1 Oligonucleotides used in hybridization experiments. Sequences underlined with same style lines (dashed or solid) are complementary to each other

Oligonucleotide	Sequence and end modifications	Total bases	Concentration in solution
Surface probe (<i>dnaK</i>)	$\text{NH}_2\text{-5}'\text{-}\underline{\text{CTTTCGCGTTGTTTGCAGAA}}$	20	$20 \mu\text{g mL}^{-1}$
Surface probe (<i>6xHis</i>)	$\text{NH}_2\text{-5}'\text{-}\underline{\text{ATGATGATGATGATGATG}}$	18	$20 \mu\text{g mL}^{-1}$
Target (<i>dnaK</i>)	$5'\text{-}\underline{\text{GTAAGTTTGAAGAGCTGGTAGAA}}$ $\underline{\text{ATGTAAGTTTGAAGAGCTGGTAC}}$ $\underline{\text{AGACTTCTGCAAACAACGCGAAAG}}$	70	1.5 μM
Sandwich probe	$\text{FITC-5}'\text{-}\underline{\text{TACCAGCTCTTCAAACCTTAC}}$	20	6 μM

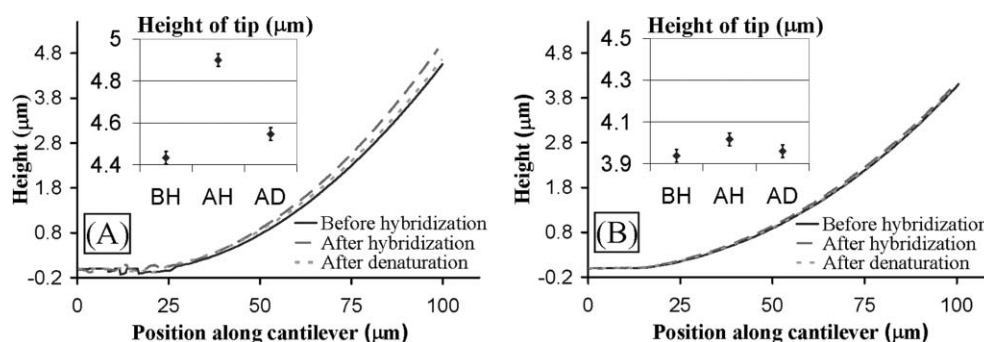


Fig. 2 (A) Vertical profile of cantilever with chitosan and *complementary* probe DNA in response to hybridization and denaturation (measured in solution). The hybridization causes upward differential bending of ~ 500 nm at the tip. The bending is reversed by denaturation. (B) Response of cantilever with chitosan and *noncomplementary* probe DNA to hybridization and denaturation (measured in solution). The differential bending is < 30 nm.

rinsing, Fig. 2A shows the cantilever's bending returns to its pre-hybridization levels. Together, the results in Fig. 2A indicate that the observed 500 nm differential bending is due to specific interactions that yield the hybridized DNA duplex.

A "control" cantilever was also tested in which the electrodeposited chitosan was functionalized with a DNA probe that is not complementary to the target. Specifically, we functionalized the film with a DNA probe to the common sequence for the hexa-histidine fusion tag (*6xHis*) and then tested this functionalized cantilever against the non-complementary *dnaK* target. No hybridization is expected for this mis-matched probe-target pair. Consistent with this expectation, Fig. 2B shows little or no change in cantilever bending upon "hybridization" and "denaturation". The small variations in this case are caused by measurement error and possibly to nonspecific DNA binding. These observations further support the conclusion that the 500 nm differential bending observed in Fig. 2A is the result of specific biomolecular interactions.

The mechanism of surface stress generation by DNA hybridization is generally not well understood. It has been explained by electrostatic and steric interactions between the DNA molecules as well as maximization of their configurational entropy,^{5,12,29,30} but comprehensive models are lacking. The generated surface stress in this study significantly exceeds

values reported in literature for DNA with similar concentration immobilized by self-assembled monolayer (SAM) techniques instead of on chitosan. We measured maximum stresses of approximately 1.5 N m^{-1} , while others report 0.02 N m^{-1} for SAMs immobilized DNA.¹⁴ The reason for this significant increase is presumably the large effective surface area of chitosan due to its 3D hydrogel structure and its high density of amine groups. We believe that micro-mechanical sensors can significantly benefit in sensitivity by the use of chitosan to immobilize the probe molecules.

3.1.2. Dynamic mode results

We also examined the potential of chitosan-coated cantilevers to mechano-transduce biomolecular recognition in dynamic mode. For dynamic analysis, DNA hybridization is detected as a change in the cantilever's resonant frequency when measurements are made in air (viscous damping dramatically reduces resonance Q factor in liquid). Typically, this resonant frequency shift is attributed to the change in mass associated with hybridization. For our studies, we electrodeposited a 100 nm film of chitosan, and functionalized it with the *dnaK* probe. This functionalized cantilever is rinsed in buffer and DI water, dried, and measured by interferometry. Fig. 3A shows the resonant frequency of the functionalized cantilever of

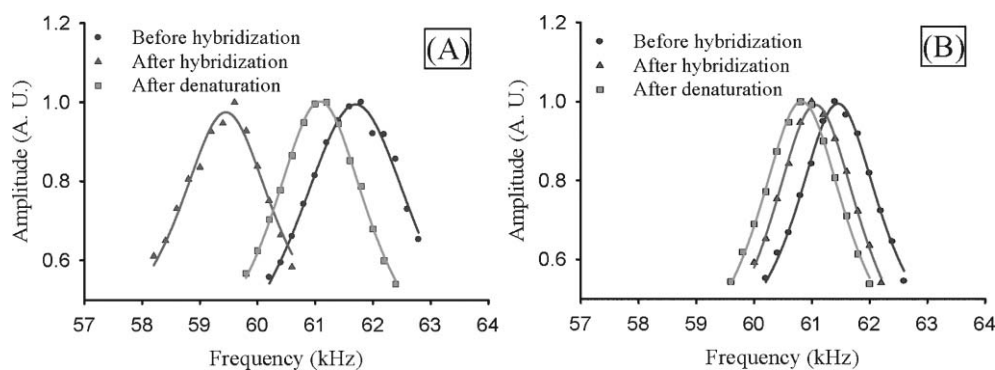


Fig. 3 (A) Frequency response of cantilever with chitosan and *complementary* probe DNA after hybridization and denaturation (measured in air). Points are raw data and curves are fitted Lorentzian functions. Hybridization reduces the resonant frequency by 2.5 kHz, and denaturation reverses the shift. (B) Frequency response of cantilever with chitosan and *noncomplementary* probe DNA after hybridization and denaturation (measured in air). Frequency shifts are < 500 Hz and are caused by humidity variation between measurements.

approximately 61.8 kHz. After measurement, the functionalized cantilever is immersed in a solution containing the complementary target DNA and allowed to hybridize for 30 min; then, the cantilever is rinsed, dried and the resonant frequency is measured. Fig. 3B shows a substantial reduction in resonant frequency to 59.4 kHz. Finally, we immerse the hybridized cantilever in a denaturing solution (4 M urea) and incubate at 80 °C for 30 min. The cantilever is then rinsed, dried, and the resonant frequency is measured again. Fig. 3A shows the resonant frequency returns to the pre-hybridized value although this return is incomplete (61.1 kHz). Presumably the observed difference in resonant frequency between the pre-hybridization and post-denaturation measurements is due either to incomplete denaturation or air humidity variations.

A control cantilever is functionalized with the noncomplementary probe (*6xHis*) and subjected to the same steps described above. Since the target and probe are mismatched in this case, minimal hybridization is expected. Fig. 3B shows the measured frequency response of the control cantilever at each step. The initial resonant frequency is 61.6 kHz. Upon hybridization, the resonant frequency becomes 61.0 kHz and upon denaturation 60.7 kHz. These differential changes in resonant frequency are small compared to the matching DNA case and are caused mainly by air humidity variations. This explanation is consistent with Fig. 3A, in which the difference between pre-hybridization and post-denaturation measurements is 0.7 kHz (ideally, it should be 0). In Fig. 3B, the corresponding difference is 0.9 kHz. Note that the complementary and noncomplementary measurements are taken within a 10 min period of each other are subject to similar environmental humidity. These results suggest that using a reference cantilever in parallel with the measurements to track instantaneous humidity variations could considerably improve the detection limit.³⁹

The DNA hybridization can affect the cantilever resonant frequency by three different mechanisms: change in the spring constant, increase in the mass, or change in the damping. Additional characterization is needed to determine the contributions of each effect to the observed resonant frequency shifts. In studies with SAMs immobilized DNA on resonators, it is typically assumed that the frequency shift is caused by

mass changes.⁴ If we assume that the mass increase effect dominates and the DNA is distributed uniformly on the cantilever, the calculated target DNA mass is approximately $16 \mu\text{g cm}^{-2}$ based on a frequency shift of 1 kHz. This is equivalent to 2.8×10^{14} target molecules cm^{-2} , two orders of magnitude over what is reported for studies using self assembled monolayers.^{14,40} This estimate is not rigorous because it has not been verified that the resonant frequency shift is caused by mass change alone and that the target DNA is uniformly distributed on the cantilever. The important observation, however, is that the frequency shift caused by hybridization of chitosan-bound DNA far exceeds that caused by self-assembled DNA. The nature of the mechanism that causes the shift is not significant for this application.

3.2. Dopamine oxidation

Our second demonstration is the mechano-transduction of an electrochemical event (*i.e.*, oxidation) used to detect the neurotransmitter dopamine selectively from ascorbic acid. As previously discussed, the products of dopamine oxidation react with the chitosan network and substantially change its mechanical properties. Chemical evidence of the reaction based on UV-Visible absorption spectra is presented in the electronic supplementary information (ESI)[†] entry for this paper. To demonstrate that the electrochemically mediated chitosan reaction can be mechano-transduced, we electrodeposit a thick chitosan film (1.5 μm) on a cantilever. The sample is placed in DI water and the initial cantilever bending is measured. Fig. 4A shows that there is initial bending because the chitosan film already has some tensile stress. The sample is then placed in an ascorbic acid solution and anodic potential is applied to the cantilever electrode, oxidizing the solution at the electrode surface. After oxidation, the sample is rinsed and placed in DI water; the cantilever bending is measured again. Fig. 4A shows small differential bending, which may be due to measurement error and nonspecific chitosan–ascorbic acid interactions.

The oxidation procedure is repeated with the same chitosan-coated cantilever in a dopamine solution. Fig. 4B shows the vertical profile of the cantilever before and after the dopamine oxidation. The cantilever bends up by approximately 800 nm

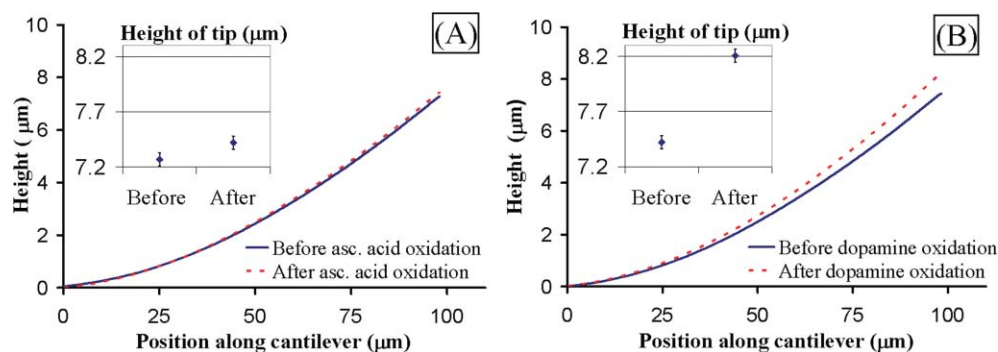


Fig. 4 (A) Response of cantilever with chitosan to *ascorbic acid* electrochemical oxidation (measured in solution). The chitosan does not react chemically. The small bending at the tip is due to measurement error and nonspecific interactions. (B) Response of cantilever with chitosan to *dopamine* electrochemical oxidation (measured in solution). The chitosan film is crosslinked and generates a tensile stress. The cantilever bends up considerably (~ 800 nm at the tip).

due to the crosslinking of chitosan by the dopamine oxidation products. The estimated stress in the chitosan film generated by the crosslinking is 1.7 MPa. These results show that the device successfully discriminates between ascorbic acid and dopamine oxidation.

It should be noted that real biological samples often contain both dopamine and ascorbic acid simultaneously, with the concentration of ascorbic acid being higher.^{33,34} Currently, our method is not capable of detecting dopamine mixed with appreciable amounts of ascorbic acid because the dopamine oxidation products are reduced by the ascorbic acid and are not allowed to react with the chitosan. In experiments where the concentration of ascorbic acid was 10 times lower than that of dopamine, the chitosan crosslinking still occurred. However, when the two concentrations were comparable, no chitosan crosslinking was observed. Well-established electrochemical methods for dopamine detection such as fast-scan cyclic voltammetry are also impacted by the interference of ascorbic acid when it is present in high concentration in dopamine samples.³³

Note also that the concentration of dopamine in our experiments (100 mM) is substantially higher than what is found in biological samples (several μM) and the detection limit has not been explored yet. Advanced cyclic voltammetry techniques are actually capable of detecting low μM concentration of dopamine.⁴¹ We envision three different strategies to enhance the sensitivity and detection limit of our sensor. First, the degree of chitosan crosslinking and the cantilever response in this work depend on the dopamine concentration and the oxidation time. For low dopamine concentrations the cantilever response can be enhanced by longer reaction times, although this would impact the temporal resolution of the detector. Second, the sensitivity of the cantilever can be further increased by reducing its spring constant to increase the bending for a given chitosan stress. Third, the interferometric measurement system in this work had large experimental error (~ 30 nm) since it was not originally designed to measure through liquid. Cantilever displacement measurements in liquid with accuracy of 0.1 nm are routinely performed using the optical lever method.⁴ This method would considerably improve the sensitivity of dopamine mechano-detection.

4. Conclusion

We report two demonstrations of the use of chitosan-coated microcantilevers for the mechano-transduction of bio-molecular and electrochemical events. In the first demonstration, hybridization of a DNA target to a chitosan-bound complementary probe was detected. The results indicate that the surface stress (observed from static measurements in solution), and the effective surface density of oligonucleotides (estimated from dynamic measurements in air) were two orders of magnitude larger than comparable observations for probes tethered to self-assembled monolayers (SAMs).^{14,40} We speculate that this greater sensitivity is due to the 3-D hydrogel nature of the chitosan film, which may allow greater probe concentrations compared to monolayer surface coverage. There was some variability in the dynamic measurements, and we attribute it to humidity effects that were not controlled

in our experimental setup. Presumably, humidity-related problems could be overcome either by carefully controlling measurement conditions or by using reference cantilevers to subtract humidity effects.

Our second demonstration was the mechano-transduction of the electrochemical oxidation of dopamine. The reaction alters the chitosan film's mechanical properties,^{31,32} and this "mechanical information" is transmitted to the cantilever. More research is needed to provide quantitative explanations for this mechano-transduction. Fortunately, chitosan does not react with oxidation products from ascorbic acid, the common interfering species in biological samples. This differential reactivity confers selectivity to the mechanical detection of dopamine, although the detection method fails if the dopamine sample has a high concentration of ascorbic acid. Potentially, the coupling of electrochemical and mechanical measurements could provide independent and complementary information that could enhance the reliability of dopamine detection in the presence of interfering chemicals.

In a broader sense, we believe chitosan is a promising material that can perform important interfacial functions: assembly (electrodeposition), functionalization (conjugation)¹⁸ and now, mechano-transduction. It is interesting to contrast the capabilities of chitosan with better-studied interfaces created through self-assembled monolayers (SAMs). SAMs *self-assemble* at the interface (typically through gold-thiol bonds), while chitosan is *directed-to-assemble* onto electrodes (often gold) in response to applied signals. SAMs form *monolayers* at the surface, while chitosan forms *3-D gel networks*. These differences may provide unique advantages for chitosan for mechano-sensor applications. Specifically, directed assembly may allow sensor addresses to be independently functionalized, while the 3-D structure may allow the generation of larger signals because more ligand can be functionalized onto the cantilever. Clearly, more work is necessary to demonstrate these potential advantages.

Acknowledgements

The authors would like to thank the Laboratory for Physical Sciences (LPS) and the National Science Foundation (NSF) for funding this work; the staff at LPS and the University of Maryland Nano Center for assistance with cleanroom facilities; and colleagues at the MEMS Sensors and Actuators Lab for useful discussions.

References

- 1 L. G. Carrascosa, M. Moreno, M. Alvarez and L. M. Lechuga, *Trends Anal. Chem.*, 2006, **25**, 196.
- 2 H. P. Lang, M. Hegner, E. Meyer and C. Gerber, *Nanotechnology*, 2002, **13**, R29.
- 3 R. McKendry, J. Zhang, Y. Arntz, T. Strunz, M. Hegner, H. P. Lang, M. K. Baller, U. Certa, E. Meyer, H.-J. Guntherodt and C. Gerber, *Proc. Natl. Acad. Sci. U. S. A.*, 2002, **99**.
- 4 N. V. Lavrik, M. J. Sepniak and P. G. Datskos, *Rev. Sci. Instrum.*, 2004, **75**, 2229.
- 5 G. Wu, H. Ji, K. Hansen, T. Thundat, R. Datar, R. Cote, M. F. Hagan, A. K. Chakraborty and A. Majumdar, *Proc. Natl. Acad. Sci. U. S. A.*, 2001, **98**.
- 6 G. Wu, R. H. Datar, K. M. Hansen, T. Thundat, R. J. Cote and A. Majumdar, *Nat. Biotechnol.*, 2001, **19**, 856.

- 7 T. L. Porter, M. P. Eastman, C. Macomber, W. G. Delinger and R. Zhine, *Ultramicroscopy*, 2003, **97**, 365.
- 8 R. L. Gunter, W. D. Delinger, T. L. Porter, R. Stewart and J. Reed, *Med. Eng. Phys.*, 2005, **27**, 215.
- 9 V. Ferrari, D. Marioli, A. Taroni, E. Ranucci and P. Ferruti, *IEEE Trans. Ultrason. Ferroelectr. Freq. Control*, 1996, **43**, 601.
- 10 M. K. Baller, H. P. Lang, J. Fritz, C. Gerber, J. K. Gimzewski, U. Drechsler, H. Rothuizen, M. Despont, P. Vettiger, F. M. Battiston, J. P. Ramseyer, P. Fornaro, E. Meyer and H. J. Guntherodt, *Ultramicroscopy*, 2000, **82**, 1.
- 11 G. Shekhawat, S. H. Tark and V. P. Dravid, *Science*, 2006, **311**, 1592.
- 12 J. Fritz, M. K. Baller, H. P. Lang, H. Rothuizen, P. Vettiger, E. Meyer, H.-J. Guntherodt, C. Gerber and J. K. Gimzewski, *Science*, 2000, **288**, 316.
- 13 K. M. Hansen and T. Thundat, *Methods*, 2005, **37**, 57.
- 14 M. Alvarez, L. G. Carrascosa, M. Moreno, A. Calle, A. Zaballos, L. M. Lechuga, C. Martinez-A and J. Tamayo, *Langmuir*, 2004, **20**, 9663.
- 15 K. M. Hansen, H. F. Ji, G. H. Wu, R. Datar, R. Cote, A. Majumdar and T. Thundat, *Anal. Chem.*, 2001, **73**, 1567.
- 16 M. Sepaniak, P. Datskos, N. Lavrik and C. Tipple, *Anal. Chem.*, 2002, **74**, 568a.
- 17 L. Q. Wu and G. F. Payne, *Trends Biotechnol.*, 2004, **22**, 593.
- 18 H. Yi, L.-Q. Wu, W. E. Bentley, R. Ghodssi, G. W. Rubloff, J. N. Culver and G. F. Payne, *Biomacromolecules*, 2005, **6**, 2881.
- 19 L.-Q. Wu, A. P. Gadre, H. Yi, M. J. Kastantin, G. W. Rubloff, W. E. Bentley, G. F. Payne and R. Ghodssi, *Langmuir*, 2002, **18**, 8620.
- 20 R. Fernandes, L.-Q. Wu, T. Chen, H. Yi, S. Li, G. W. Rubloff, R. Ghodssi, W. E. Bentley and G. F. Payne, *Langmuir*, 2003, **19**, 4058.
- 21 L.-Q. Wu, H. Yi, S. Li, G. W. Rubloff, W. E. Bentley, R. Ghodssi and G. F. Payne, *Langmuir*, 2003, **19**, 519.
- 22 H. Yi, L.-Q. Wu, R. Ghodssi, G. F. Payne and W. E. Bentley, *Langmuir*, 2005, **21**, 2104.
- 23 J. Redepenning, G. Venkataraman, J. Chen and N. Stafford, *J. Biomed. Mater. Res. A*, 2003, **66**, 411.
- 24 L. Q. Wu, K. Lee, X. Wang, D. S. English, W. Losert and G. F. Payne, *Langmuir*, 2005, **21**, 3641.
- 25 X. L. Luo, J. J. Xu, Y. Du and H. Y. Chen, *Anal. Biochem.*, 2004, **334**, 284.
- 26 M. J. Kastantin, S. Li, A. P. Gadre, L. Q. Wu, W. E. Bentley, G. F. Payne, G. W. Rubloff and R. Ghodssi, *Sens. Mater.*, 2003, **15**, 295.
- 27 H. Yi, L.-Q. Wu, R. Ghodssi, G. W. Rubloff, G. F. Payne and W. E. Bentley, *Anal. Chem.*, 2004, **76**, 365.
- 28 H. Yi, S. Nisar, S.-Y. Lee, M. A. Powers, W. E. Bentley, G. F. Payne, R. Ghodssi, G. W. Rubloff, M. T. Harris and J. N. Culver, *Nano Lett.*, 2005, **5**, 1931.
- 29 R. Mukhopadhyay, M. Lorentzen, J. Kjems and F. Besenbacher, *Langmuir*, 2005, **21**, 8400.
- 30 W. Shu, D. Liu, M. Watari, C. K. Riemer, T. Strunz, M. E. Welland, S. Balasubramanian and R. A. McKendry, *J. Am. Chem. Soc.*, 2005, **127**, 17054.
- 31 L.-Q. Wu, R. Ghodssi, Y. A. Elabd and G. Payne, *Adv. Funct. Mater.*, 2005, **15**, 189.
- 32 L.-Q. Wu, M. K. McDermott, R. Ghodssi and G. F. Payne, *Adv. Funct. Mater.*, 2006, **16**, 1967.
- 33 B. J. Venton and R. M. Wightman, *Anal. Chem.*, 2003, **75**, 414A.
- 34 L. Zhang and X. Jiang, *J. Electroanal. Chem.*, 2005, 292.
- 35 S. D. Senturia, *Microsystem Design*, Kluwer Academic Publishers, Dordrecht, the Netherlands, 2001.
- 36 S. A. Smee, M. Gaitan, D. B. Novotny, Y. Joshi and D. L. Blackburn, *IEEE Electron Device Lett.*, 2000, 21.
- 37 Y. Zhang, Q. Ren and Y.-P. Zhao, *J. Phys. D: Appl. Phys.*, 2004, **37**, 2140–2145.
- 38 J. E. Sader, *J. Appl. Phys.*, 2001, 89.
- 39 K. Y. Gfeller, N. Nugaeva and M. Hegner, *Biosens. Bioelectron.*, 2005, **21**, 528.
- 40 T. H. Ha, S. Kim, G. Lim and K. Kim, *Biosens. Bioelectron.*, 2004, **20**, 378.
- 41 B. J. Venton, K. P. Troyer and R. M. Wightman, *Anal. Chem.*, 2002, **74**, 539.